Aeronomic Systems on Planets, Moons, and Comets

Darrell F. Strobel

Departments of Earth and Planetary Sciences and Physics and Astronomy, The Johns Hopkins University

This chapter provides a basic introduction to the science of aeronomy and a comparison of aeronomic systems for planets, satellites, and comets in our solar system. The fundamental length scales of scale height, mean-free-path, and depletion length are introduced, along with the non-dimensional parameters, Mach number, the Jeans' λ ratio of gravitational potential energy to random kinetic energy, and the ratio of mean-free-path to scale height. These quantities are used to define exobase and the validity of the fluid approximation for a gas and to classify atmospheres, exospheres and comas. Planetary and satellite atmospheres are also classified by their chemical composition and photochemistry is addressed within these categories. The thermal structure of thermospheres is reviewed and the role of molecular heat conduction is emphasized. It is noted that solar heating is an insignificant thermospheric heat source on the giant planets. The general importance of wave heating is scrutinized, specifically the question is posed: why don't all planetary atmospheres have hot coronas?

1. INTRODUCTION

When a gas is bound gravitationally to a planetary or satellite solid "nucleus", it is defined to be an atmosphere. If the gas is not restricted by gravity, it is called a coma. In the case of the giant planets the "nuclei" are rocky cores on the order of 0.1 radii and the gas constitutes most of the planet. Most planets and many satellites in our solar system are surrounded by gravitationally bound atmospheres. The presence or absence of an atmosphere is an important characteristic of a planet or satellite. Why does Ganymede, the largest satellite, have an atmosphere of 10^{-12} bar, whereas slightly smaller Titan has a denser atmosphere than the Earth of 1.4 bar? Comets cannot retain gases by gravity and thus have comas. The coma is due to evaporation of nuclear ice, principally water ice for solar distances less than 3 AU, and its abundance is directly related to the evaporation rate driven by the solar radiation field. In the evaporation process considerable dust can be ejected from the nucleus.

Atmospheres in the Solar System: Comparative Aeronomy
Geophysical Monograph 130

10.1029/130GM02

2. NOMENCLATURE

While there is no universally accepted definition of the word, aeronomy, the *American Heritage Dictionary* defines it as "The study of the upper atmosphere, especially of regions of ionized gases". *Sydney Chapman* [1960] defined aeronomy as "the science of the upper region of the atmosphere, where dissocation and ionization are important". Aeronomy, from a historical perspective, is the science of atmospheric regions where dissociation and ionization are important factors in understanding composition and structure. In the Earth's

atmosphere the photochemistry of molecular oxygen leads to the formation of ozone. Ozone photochemistry results in the atmospheric heating and formation of the stratosphere. Traditionally the word, aeronomy, is synonymous with upper atmosphere, whereas a strict application of its definition could include the entire atmosphere as dissociation is also an important factor in the chemistry of the Earth's lower atmosphere known as the troposphere (see Figure 1).

The troposphere is characterized by a relatively constant negative temperature gradient, $\sim$ - 6.5 K km^{-1}. The boundary between the stratosphere, which has a positive temperature gradient $\sim$ 2 K km^{-1}, and the troposphere is the tropopause. Continuing atmospheric nomenclature based on temperature profile, we have a mesosphere above the stratosphere with a boundary known as the stratopause. The mesosphere is characterized by a negative temperature gradient of $\sim$ - 3 K km^{-1}, which is produced by ozone heating and CO_2 infrared cooling and a direct consequence of the observed O_3/CO_2 density ratio decreasing with height. Above the mesosphere, with its upper boundary known as the mesopause, is the thermosphere which is characterized by a very rapid temperature increase of $\sim$ 10-20 K km^{-1}, at low altitudes and asymptotically approaches a constant (isothermal) temperature at high altitudes. The basic physics of the thermosphere is intense heating by absorption of short wavelength solar ultraviolet radiation (< 170 nm) in the dissociation and/or ionization of molecules and atoms and the downward transport of thermal energy by heat conduction to infrared active molecules, such as CO_2, capable of radiating thermal energy away. Although this nomenclature is based on the Earth's temperature profile, it is adopted for other atmospheres, even if the physics generating their temperature profiles, illustrated in Fig. 1, may be dominated by different processes. The asymptotic isothermal thermospheric temperatures are given in Table 1.

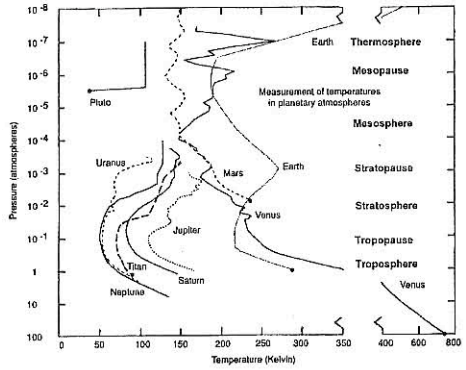

Figure 1. Nomenclature based on the U. S. Standard Atmosphere for the Earth. Temperature profiles as a function of pressure for other planetary atmospheres are based on in situ descent probes (Venus and Mars) and ground-based and spacecraft occultation data for the other planets and satellites. Small scale wave-induced temperature oscillations have been retained. Surface values are indicated by solid circles. Note temperature scale discontinuity between 350 and 400 K. This figure is based on Figure 4.4 from An Integrated Strategy For The Planetary Sciences 1995-2010, National Academy Press, Washington, DC, and used with permission.

3. FUNDAMENTAL LENGTH SCALES AND DEFINITIONS

The atmosphere can be treated as a fluid in part because the mean free path, the distance a molecule or atom travels before making a collision, is much shorter than the smallest macroscopic length scale, which is the pressure scale height, H, that characterizes the exponential decay of pressure with altitude (for the Earth, H = 8 km at the surface, where the mean free path is $\sim 10^{-5}$ cm). Individual atoms and molecules undergo many collisions in macroscopic time scales and in a volume H^3 there are a huge number of atoms and molecules that, for all macroscopic purposes, the atmosphere can be viewed as a continuum fluid.

The mean free path varies inversely as the number density and there will be some altitude ($\sim$ 450 km for the Earth's atmosphere) where the mean free path is approximately equal to the atmospheric scale height . This level, defined rigorously below, is known as the exobase and the region above the exobase is known as the exosphere. Because the exosphere has a larger mean free path than scale height, it is regarded as a quasi-collisionless region and discussed in Chapters III.2 and III.3.

To understand the physical significance of the exobase on escaping atoms and molecules and the distinction between an atmosphere and an exosphere, let us focus on the atmosphere at the exobase. The collision cross section for an atom/molecule may be defined as $\sigma = \pi d^2$, where d is the atomic/molecular diameter, because a collision occurs if the atoms or molecules touch in the rigid sphere limit. A typical value for σ is $\sim$ (3 - 4)

Table 1. General Properties of Atmospheres/Exospheres/Comas Around Solar System Objects

Atmospheric Type	Object	Main Composition	P, T at surface or 1 bar	T_∞	$\lambda_{1\ \mu bar}$	$\lambda_{exobase}$	Exobase Height (km), $r_{exobase}/r_n$	Escaping Constituents	Solar EUV, Particle/Joule Heating (10^9 W)
H_2-He atmospheres of the giant planets	Jupiter	H_2, He, CH_4, NH_3	1 bar, 165 K	900 K	2300	480	1600, 1		800,10^5
	Saturn	H_2, He, CH_4, NH_3	1 bar, 160 K	420 K	1300	420	2500, 1		200, 200
	Uranus	H_2, He, CH_4, NH_3	1 bar, 80 K	870 K	200	50	4700, 1.2		8, 100
	Neptune	H_2, He, CH_4, NH_3	1 bar, 80 K	600 K	450	120	2200, 1.1		3, 1
Terrestrial CO_2 atmospheres	Venus	CO_2, N_2, SO_2, Ar	90 bar, 730 K	200 K	1600	35	140, 1	H	300, -
	Mars	CO_2, N_2, Ar, O_2	7 mbar, 220 K	300 K	490	200	160, 1.1	H, H_2, O, N	25, -
N_2 atmospheres	Earth	N_2, O_2, Ar, H_2O	1 bar, 280 K	1000 K	1100	130	450, 1.1	H	500, 80
	Titan	N_2, CH_4, H_2	1.4 bar, 94 K	160 K	68	45	1500, 1.6	H, H_2, N	3, < 0.2
	Triton	N_2, CO, CH_4, H_2	14 µbar, 38 K	100 K	84	23	930, 1.7	H, H_2, N	0.05,0.1
	Pluto	N_2, CO, CH_4, H_2	3-90 µbar, 35-45 K	?	21	?	> 3000, > 3	N_2, CH_4, H, H_2	0.05, ?
Volcanic atmospheres	Io	SO_2, S_2, SO, O	0.3 nbar, 120 K	2000 K	NA	9	500, 1.3	O, S, Na	< 2, 400
Sputter generated atmospheres	Europa	O_2, O, H_2O	0.7 pbar, 100 K	1000 K?	NA	8	30, 1	O_2, O, H, H_2	0.1, 30
	Ganymede	O_2, O, H_2O	0.7 pbar, 120 K	1000 K?	NA	?	30, 1	O_2, O, H, H_2	0.3, ?
	Callisto?	CO_2, O_2, O, H_2O	0.7 pbar, 150 K	?	NA	?	30, 1		0.2, ?
	Moon	Ar, Na, K			NA		0, 1		
	Mercury	Na, K, Ca			NA		0, 1		
Comas	Comets	H_2O, CH_4, CO, CO_2, CH_3OH			NA		NA	H_2O, H, OH, O	
	Chiron	CO?			NA		NA	CO	

x 10^{-15} cm^2. Thus the exobase of a planet/satellite with radius, r_p, is rigorously defined as the height, $z_{exobase} = r_{exobase} - r_p$, where the probability for an atom or molecule traveling upward with speed in excess of the escape velocity is e^{-1} for escape without suffering a collision and given by

$$\text{Probability} = exp\left(-\int_{z_{exobase}}^{\infty} \sigma n(z)dz\right) \quad (1)$$
$$= exp(-\zeta(z_{exobase})^{-1}) = e^{-1}$$

where $\zeta(z) = (\sigma n(z)H(z))^{-1}$. Here $n(z)$ is the total number density. Note that the quantity $\zeta(z)$ in Eq. (1) is a parameter that describes the validity of treating the atmosphere as a fluid and collision-dominated gas. It is rigorously a fluid when $\zeta \ll 1$. At the exobase $\zeta = 1$ and the mean free path, $l(z)$ equals

$$l(z) = \frac{H}{\sqrt{2}} \quad (2)$$

where

$$\text{mean free path} = l(z) = \frac{\zeta(z)H(z)}{\sqrt{2}},$$
$$\text{and scale height} = H(z) = \frac{kT(z)}{mg(z)}.$$

Here $T(z)$ is the temperature, m is the mean mass of atoms and molecules, g is the gravitational acceleration $= GM_p/r^2$, where the total mass of the planet/satellite is M_p, and G = Newton's gravitational constant. Note that in this chapter height z and radius r will be used interchangeably for the independent radial variable. Exobase heights are given in Table 1.

4. FIVE BASIC PARAMETERS FOR A CLASSIFICATION SCHEME OF ATMOSPHERES, COMAS, AND EXOSPHERES

The most idealized, gravitationally bound atmosphere would be one in which the thermal escape rate is precisely zero. Although this limit is unattainable, it is instructive to examine the factors that govern thermal escape to understand what constitutes an atmosphere. In the classic model for atmospheric escape one assumes that the atmosphere at and below the exobase is fully collisional and atoms and molecules have a Maxwellian distribution of velocities with a sharp transition to a collisionless exosphere just above the exobase. The escape flux due to thermal evaporation from an atmosphere with exobase density, n, is given by the classic Jeans formula (see discussions in Chapters III.2 and III.3)

$$F_{esc}(r_{exobase}) = \frac{n(r_{exobase})U}{2\sqrt{\pi}}(\lambda + 1)exp(-\lambda) \quad (3)$$

in terms of a non-dimensional quantity evaluated at the exobase $\lambda = v_{esc}^2/U^2$, where U is the most probable velocity of a Maxwellian distribution given by

$$U = \left(\frac{2kT}{m}\right)^{\frac{1}{2}} \quad (4)$$

and the escape velocity at the exobase from the planet/satellite's gravitational potential well, v_{esc}, is defined as

$$v_{esc}(r_{exobase}) = \left(\frac{2GM_p}{r_{exobase}}\right)^{\frac{1}{2}} \quad (5)$$

The physical significance of λ can be appreciated by rewriting it as follows:

$$\lambda(r_{exobase}) = \frac{v_{esc}^2}{U^2} = \frac{\frac{GM_p m}{r_{exobase}}}{kT} \quad (6)$$
$$= \frac{\text{gravitational potential energy}}{\text{random kinetic energy}} = \frac{r_{exobase}}{H}$$

Thus in the limit $\lambda \to 0$ the atmosphere is no longer gravitationally bound and blows away due to immense random kinetic energy, whereas in the limit of large λ the atmosphere is gravitationally retained and thermal escape is negligible ($\lambda \to \infty$ being the idealized limit of no escape). The coma of a comet represents the former case, while Jupiter is an excellent example of the latter. Table 1 gives representative values of λ at the exobase for the dominant atmospheric constituent at this height for many solar system objects. Note that atmospheres with small values of λ at the exobase also have the most extended atmospheres, "large" values of $r_{exobase}/r_p$. For example in the category of the giant planets, Uranus has 1.2 for this ratio and only 50 for λ at the exobase in comparison to ~ 1 and 480 for Jupiter. Titan and Triton also have more extended atmospheres of 1.6 and 1.7, respectively, with exobase λs' of 45 and 23. In addition, λ is also evaluated at the 1 μbar level, typically the mesopause region, to give a further indication of how strongly various atmospheres are gravitationally bound at higher pressures. Note that Pluto has the least gravitationally bound atmosphere of any object that possesses a surface pressure of at least 1 μbar. It is highly probable that $r_{exobase}/r_p > 3$ for Pluto, if its 1 μbar temperature of 100 K extends isothermally up to the exobase.

The limit $\lambda \to 0$, is known as the Jeans limit and is the maximum thermal escape rate

$$\lim_{\lambda \to 0} F_{esc}(r_{exobase}) = \frac{n(r_{exobase})U}{2\sqrt{\pi}} \quad (7)$$
$$= \tfrac{1}{4}n(r_{exobase})v_{thermal}$$

where $v_{thermal} = \left(\frac{8kT}{\pi m}\right)^{\frac{1}{2}} = 1.13U$
which is simply the upward directed thermal flux at the exobase that one could calculate from simple kinetic theory. Note that the λ parameter in Eq. (3) is linearly proportional to the particle mass and thus light constituents will have much higher escape rates and larger scale heights than heavy constituents. In Table 1 constituents that have significant escape rates from solar system objects are listed.

In order to further clarify the classification and distinction among atmosphere, exosphere, and coma, we explore analytic solutions to the equations of continuity and motion or momentum in the radial direction [*Summers et al.*, 1989]. From standard textbooks on fluid dynamics (e. g. *Landau and Lifshitz*, 1959), the momentum equation in the radial direction, r, can be written as

$$\frac{\partial}{\partial r}\left(\frac{1}{2}w^2\right) + \frac{1}{\rho}\frac{\partial p}{\partial r} + \frac{GM_p}{r^2} = 0 \quad (8)$$

where p = pressure, ρ = nm = mass density, w = radial velocity, r = radial distance from the center of the object. For an isothermal atmosphere this equation may be rewritten as

$$\frac{\partial}{\partial r}\left(\frac{w}{U}\right)^2 + \frac{1}{n}\frac{\partial n}{\partial r} - \frac{\partial \lambda}{\partial r} = 0 \quad (9)$$

and integrated to give

$$n(r) = n(r_0)exp[(\lambda(r) - \lambda_0(r_0)) - (M(r) - M_0(r_0))] \quad (10)$$

where $M(r) = \left(\frac{w(r)}{U}\right)^2$
with boundary conditions specified at some appropriate level r_0 and the density $n(r)$ and radial velocity $w(r)$ are subject to the constraint imposed by the continuity equation, e.g., in the absence of chemistry, $4\pi r^2 n(r)w(r)$ is a constant. Equation (10) illustrates a number of interesting properties. In the limit of no radial flow ($M(r) = M_0(r_0) = 0$), one obtains hydrostatic equilibrium for a gravitationally bound gas where the downward gravitational force is precisely balanced by an upward pressure gradient force

$$n(r) = n(r_0)exp(\lambda(r) - \lambda_0(r_0)) \quad (11)$$
$$= \lim_{H/r_p \to 0} n(r_0)exp\left(-\tfrac{r-r_0}{H}\right)$$

where the right hand limit holds for atmospheres with small scale heights in comparison to the radius of the planet or satellite, r_p. The scale height H is just the radial, e-folding, macroscopic length scale of pressure. In the limit of rapidly increasing radial flow at large r, Eq. (10) implies the density profile will decrease more rapidly with r than the "no flow" limit. This additional decrease is modest for subsonic flows ($M(r) \ll 1$). To achieve dramatic decreases in density, high Mach number ($M(r) \gg 1$) flows are required, as characteristic of the sun's solar wind and the Earth's polar wind.

With radial outflow, the importance of net loss/ production processes must be evaluated. Loss processes that are far more consequential include thermal ion sputtering of the neutral atmosphere, electron impact ionization, and electron impact dissociation into fast escaping atoms, and charge exchange, all of which are especially relevant for satellites embedded in magnetospheric plasma. Specifically for the Galilean satellites Io and Europa, the loss or residence times for their atmospheres are only 2-3 days [*Strobel and Wolven*, 2001].

In steady-state with a net loss rate, L, the continuity equation for spherically symmetric radial outflow is

$$\frac{\partial}{\partial r}(r^2 n_2 w) = -Ln \quad (12)$$

If L and w are constant (L_0, w_0), then the solution to Eq. (12) is

$$n(r) = n_0(r_0)\left(\frac{r_p}{r}\right)^2 exp\left[-\left(\frac{L_0}{w_0}\right)(r - r_0)\right] \quad (13)$$

where $r - r_0 = z$ is the height above the surface. One can define a depletion length scale or scale height associated with this coronal loss model [*Summers et al.*, 1989] as

$$H_d = \left(\frac{-1}{n}\right)\left(\frac{dn}{dr}\right) \approx \frac{w_0}{L_0} \quad (14)$$

where expression (13) has the following desirable properties. For very large H_d due to either large w_0 and/or very small L, the radial density profile yields the radial outflow solution for a cometary coma in which $4\pi r^2 n w_0$ is a constant. In the other limit of negligible w_0 and/or large L such that $H_d/r_p \ll 1$, the radial density profile is dominated by the exponential term and corresponds to an isothermal atmosphere with constant gravitational acceleration.

Thus we have five basic parameters ($\zeta, \lambda, M, H, H_d$) to classify gaseous envelopes around solar system objects into atmospheres, exospheres, and comas. To be classified as an atmosphere, $0 < \zeta(r) < 1$ and λ must be large ($\gg 1$), whereas when $\zeta(r) > 1$ with large λ, it

is an exosphere. The importance of exospheric loss processes is indicated by the ratio of H_d/H being ≤ 1. For a cometary coma near the surface $\lambda \ll 1, M \sim 1, H \to \infty$, and H_d is the relevant macroscopic length scale ($\sim 10^6$ km) with L_0 essentially equal to the H_2O photodissociation rate and $w_0 \sim 1$ km s^{-1}. For subliming gases vaporization theory predicts mean efflux velocity bounded by $0.565U \leq v_e \leq 0.75U$ [*Delsemme and Miller*, 1971]. Adiabatic expansion into a vacuum with conversion of accessible enthalpy into radial kinetic energy yields for water a terminal gas velocity of 2U, which is 2.5 times the sonic velocity for water, for a ratio of specific heats, $\gamma = 1.33$. For bright comets at 1 AU, a typical water gas production rate is $Q \sim 10^{30}$ molecules s^{-1}, with radial velocity, $v_r = 2U \sim 1$ km s^{-1}, $\lambda \sim 4$ x 10^{-6}, and approximate radial density distribution for a spherically symmetric nucleus, R_c, given by

$$n(r) = \left(\frac{Q}{4\pi R_c^2}\right)\frac{R_c^2}{v_r r^2} \tag{15}$$

with mean free path from Eq. (2) of

$$l(r) = \frac{2\sqrt{2}\pi r^2}{\sigma Q}.$$

With $R_c \sim 2$ km, $l \sim 10$ cm at the surface and ~ 5 x 10^4 km at a radial distance of 5 x 10^4 km. The collision zone of a coma extends to a distance where $l(r) \sim r$. This defines the outer boundary of the inner coma (the coma's equivalent to an exobase).

While the classifications of atmospheres and comas is straightforward for very small and very large values of λ, the most difficult λ domain is for $\lambda \sim 1$, where the atmosphere is in hydrodynamic escape or blowoff. Unfortunately, an analytic description of a hydrodynamically escaping atmosphere has so far been elusive. Although no solar system atmosphere has been proven to be hydrodynamically escaping, Pluto's atmosphere is widely believed to exhibit the requisite conditions. For an isothermal atmosphere, Eq. (9) can be combined with the continuity equation for lossless radial outflow, $4\pi r^2 n(r) w(r) = 4\pi r^2 n(r) M(r) U =$ constant to obtain

$$(2M^2 - 1)\frac{\partial}{\partial r}(lnM) - \frac{2}{r} - \frac{\partial \lambda}{\partial r} = 0 \tag{16}$$

with a sonic point at $M = 1/\sqrt{2}$. If the sonic point were at the exobase with $\lambda = 1/2$, then the radial outflow velocity, w, equals $U/\sqrt{2}$ and the escape velocity. This result may be compared with the Jeans escape flux per unit density from a hydrostatic (no radial flow) atmosphere with $\lambda = 1/2$ in Eq. (3) which yields

$$\frac{F_{esc}(r_{exobase})}{n(r_{exobase})} = \frac{0.91U}{2\sqrt{\pi}} = \frac{0.91}{4} v_{thermal} = 0.36 v_{esc} \tag{17}$$

which is 91% of the Jeans limit ($\lambda \to 0$).

An alternate and more conservative threshold for onset of hydrodynamic escape is based on energy considerations and can be inferred from the continuity equation for radial flow in the absence of chemistry, $4\pi r^2 \rho(r) w(r)$ = constant, and the steady state equation for conservation of total energy for an ideal gas

$$\nabla \cdot \left[\rho \vec{v}\left(\tfrac{1}{2}\vec{v}\cdot\vec{v} + h\right) - \vec{v}\cdot\acute{\sigma}_{ik} - \kappa\nabla T\right] = Q + \rho\vec{v}\cdot\vec{F} \tag{18}$$

where h is the enthalpy of gas $= c_p T$, Q is the internal heating, κ is the thermal conductivity, $\acute{\sigma}_{ik}$ is the viscous stress tenor, and $\vec{F}$ is the external force(s) on the fluid, assumed here to be written as the gradient of potential field(s), with $-\nabla\Phi_g$ for gravity. In a conservative, dissipationless atmosphere, $\acute{\sigma}_{ik} = \kappa = Q = 0$, and the conservation of total energy reduces to, with the aid of the continuity equation $\nabla \cdot (\rho\vec{v}) = 0$,

$$\nabla \cdot \left[\rho\vec{v}\left(\frac{1}{2}\vec{v}\cdot\vec{v} + h + \Phi_g\right)\right] = 0 \tag{19}$$

and becomes for radial flow

$$r^2 \rho w = \text{constant}, \left(\frac{1}{2}\vec{v}\cdot\vec{v} + h + \Phi_g\right) = \text{constant} \tag{20}$$

which is Bernoulli's equation for potential flow of a compressible gas. At some very low altitude, $z = z_0$, $\frac{1}{2}\vec{v}\cdot\vec{v} \ll h$ and the constant in the last equation is effectively $= h_0 + \Phi_{g0}$. If $w(\infty) > 0$, then the atmosphere is escaping. The threshold conditions for atmospheric blowoff are $w(\infty) = 0$ at z or $r \to \infty$ and $h_0 = -\Phi_{g0}$, where the enthalpy of the atmosphere is converted into directed radial outflow kinetic energy which in turn is converted into gravitational potential energy. The condition $h_0 = -\Phi_{g0}$ can be rewritten as

$$\frac{\frac{GM_p}{r_0}}{c_p T_0} = \frac{R\lambda_0}{c_p} = 1 \tag{21}$$

where it is assumed that as the atmosphere expands into a vacuum its internal energy is accessible and convertible into translational energy with escape velocity $w_{esc} = (c_p/R)^{1/2}U$. For atmospheric atoms $c_p = 5/2R, w_{esc} = 1.6U, \lambda_0 = 5/2$, and for molecules N_2, O_2, $c_p = 7/2R, w_{esc} = 1.8U, \lambda_0 = 7/2$, where the gas constant $R = k/m$. The atmospheric molecules H_2 (giant planets) and CO_2 (Venus and Mars) have temperature dependent specific heats as not all rotational energy levels are populated in H_2 and some vibrational levels are populated in CO_2 at relevant atmospheric temperatures.

In a real atmosphere with internal heating and dissipation, hydrodynamic escape requires a continual source of power to replenish the enthalpy of the atmosphere and maintain atmospheric blowoff. For the terrestrial planets, the most probable power source would be solar EUV and UV heating. On the giant planets atmospheric blowoff was probably never important. Pluto is one planet where conditions may currently be favorable for hydrodynamic escape and certainly Triton, Titan, and the Galilean satellites with their weak gravity and extended atmospheres have potential for rapid escape. Current estimates for the residence times of the atmospheres of Io and Europa are only 2-3 day [*Strobel and Wolven*, 2001] based on the canonical escape rate for Io of 1.6 x 10^{28} SO_2 molecules s^{-1} and the calculated removal rate of $\sim$ 1 x 10^{27} O_2 molecules s^{-1} from Europa's atmosphere [*Saur et al.*, 1998]. At their exobases, their radial outflow speeds are ~ 0.05U and 0.001U, respectively.

5. VERTICAL STRUCTURE: DIFFUSION AND MIXING

In the lower region of a planetary atmosphere known as the homosphere, chemical tracers are observed to have quasi-constant volume mixing ratios, μ_i (ratio of individual number density, n_i, to total number density, N). This property is due to the action of mean winds and atmospheric waves in the presence of some form of "dissipation", i.e. external solar heating, mechanical friction, IR radiative cooling and damping, finite chemical lifetime, which renders the atmosphere nonconservative. For example, a linear, conservative wave just oscillates a parcel of air back and forth without any net displacement or transport. The presence of active chemistry can generate net transport. Mathematically this tendency may be expressed by the globally averaged, vertical continuity equation as

$$\frac{\partial \mu_i}{\partial t} = \frac{1}{N}\frac{\partial}{\partial z}\left(NK_{zz}\frac{\partial \mu_i}{\partial z}\right)$$

where K_{zz} is the vertical eddy diffusion coefficient [*Colegrove et al.*, 1966].

In the upper atmosphere the tendency for chemical tracers in the limit of negligible chemical loss is towards a balance between a downward gravitational force and an upward partial pressure gradient force. The resulting height distribution is an exponential decrease in density with height based on tracer's scale height which is inversely proportional to its mass. This force balance is known as gravitational diffusive equilibrium. The homopause is the transition region from the well-mixed homosphere below, where chemically inert tracers tend to have constant mixing ratios, to the heterosphere above where tracers asymptotically approach gravitational diffusive equilibrium density profiles. Transport in the heterosphere is dominated by molecular diffusion, represented by coefficients D_i and D_{ij}. This tendency toward gravitational diffusive equilibrium in the heterosphere may be similarly expressed in the globally averaged, vertical continuity equation for minor constituents as

$$\frac{\partial \mu_i}{\partial t} = \frac{1}{N}\frac{\partial}{\partial z}\left\{D_i N\left[\frac{\partial \mu_i}{\partial z} + \left(\frac{1}{H_i} - \frac{1}{H}\right)\mu_i\right]\right\} + \frac{1}{N}\frac{\partial}{\partial z}\left\{K_{zz} N \frac{\partial \mu_i}{\partial z}\right\}$$

where

$$D_i^{-1} = \sum_{j \neq i}\frac{n_j}{N D_{ij}}, \text{and } D_{ij} = \frac{b_{ij}}{N}$$

Low in the atmosphere $D_i/K_{zz} \ll 1$, and molecular diffusion may be neglected. High in the atmosphere $D_i/K_{zz} \gg 1$ since $D_i \propto N^{-1}$. The transition level where $D_i = K_{zz}$ is the formal definition of the homopause. The application of the kinetic theory of molecular diffusion coupled with eddy diffusion to atmospheric transport was discussed by *Colegrove et al.* [1966].

For a minor constituent in an isothermal atmosphere with no chemistry and no net flux, the two tendency equations can be combined and integrated to yield the following steady-state, static solution [*Chamberlain and Hunten*, 1987].

$$\mu_i = (1 + e^{h/H})^{1 - \frac{H}{H_i}}\mu_{0i}$$

where the homopause location, $h = 0$ is given by $D_i = K_{zz}$ with homopause density $N_0 = b_i/K_{zz}$. The solution has the following respective limits:

$$\mu_i \to \mu_{0i}, h \to -\infty$$
$$\mu_i = 2^{1 - \frac{H}{H_i}}\mu_{0i}, h = 0$$
$$\mu_i \to \mu_{0i} exp\left[-h\left(\frac{1}{H_i} - \frac{1}{H}\right)\right], h \to +\infty$$

Deep in the atmosphere the mixing ratio is μ_{0i}. At the homopause the mixing ratio can be considerably smaller than its deep atmosphere value, if the specie i is much heavier than the mean molecular mass of the background atmosphere, as is true for hydrocarbons in the atmospheres of the giant planets. High in the heterosphere, light species relative to major atmospheric constituents have increasing mixing ratios, whereas heavy species have decreasing mixing ratios.

6. COMPOSITION AND CHEMISTRY

Planetary and satellite atmospheres may also be classified by their chemical composition. The major types are the H_2-He atmospheres of the giant planets, the terrestrial CO_2 atmospheres, and the N_2 atmospheres of Earth, Pluto, Titan, and Triton. In addition to these categories there are the volcanic generated SO_2 atmosphere of Io, tenuous sputter-generated O_2 atmospheres on Europa and Ganymede, a CO_2 atmosphere on Callisto, and exospheres on Mercury and the Moon.

6.1. H_2-He Atmospheres

The atmospheres of the giant planets are predominantly molecular hydrogen ($\sim$ 85-95% by number) with the remainder mostly helium. Trace amounts of the saturated hydrides (CH_4, NH_3, H_2O, H_2S) of reactive atoms of cosmically abundant elements C, N, O, S are present in the deep atmospheres of the giant planets, as predicted by thermochemistry to be the dominant form of these elements. These hydrides are also the condensible substances for cloud formation. The working hypothesis for the formation of the solar system is the nebular hypothesis which first gained prominence in the writings of Kant and Laplace. The giant planets got a head start in the cooler nebular regions of the outer solar system. Solids condensed first there and subsequently collided, aggregated, and eventually became self-gravitating protoplanets sweeping up neighboring solids gravitationally and capturing H_2 and He gases in roughly solar proportions. The enhanced abundances of saturated hydrides over expectations based on solar elemental ratios (factors of 3 for Jupiter and Saturn and factors of 30 for CH_4 on Uranus and Neptune) have been measured in situ by the Galileo probe in Jupiter's atmosphere and by remote sensing on all the giant planets. These enhanced abundances are attributed to condensation of solids (the saturated hydrides) as the seed nuclei that initiated the formation process of the giant planets. Some enrichment would be predicted as 100% capture of surrounding H_2 and He gases would be improbable.

Some trace species in the upper atmospheres of the giant planets (e. g. C_2H_6, C_2H_2, C_2H_4, C_4H_2,) are too abundant to have a thermochemical origin, even if they were convected from the deep, hot interior. These species are best understood as the products of CH_4 photochemistry. The photochemistry of inorganic compounds, NH_3 and PH_3, and the formation of condensible N_2H_4 and P_2H_4 may contribute along with polyacetylenes and other hydrocarbons to the ubiquitous haze in the tropopause regions of the Jupiter and Saturn. The external (to the planet/satellite) introduction of matter by infall of meteoroids and material from rings and satellites containing oxygen leads to the photochemical formation of CO and CO_2.

The photochemistry of H_2 and He leads to the formation of ionospheres on the giant planets

$$H_2 + h\nu \rightarrow H_2^+ + e \text{ or } H + H^+ + e;$$
$$\mathrm{I} = 5.4 \times 10^{-8}, 9.5 \times 10^{-9}\ \mathrm{s}^{-1} \text{ at 1 AU}$$
$$H + h\nu \rightarrow H^+ + e\ ;\ \mathrm{I} = 7.3 \times 10^{-8}\ \mathrm{s}^{-1} \text{ at 1 AU}$$
$$He + h\nu \rightarrow He^+ + e\ ;\ \mathrm{I} = 5.2 \times 10^{-8}\ \mathrm{s}^{-1} \text{ at 1 AU}$$
$$H_2^+ + H_2 \rightarrow H_3^+ + H\ ;\ \mathrm{k} = 2 \times 10^{-9}\ \mathrm{cm}^3\ \mathrm{s}^{-1}$$
$$He^+ + H_2 \rightarrow HeH^+ + H\ ;\ \mathrm{k} = 4.2 \times 10^{-13}\ \mathrm{cm}^3\ \mathrm{s}^{-1}$$

and when the plasma recombines the production of H atoms

$$H_3^+ + e^- \rightarrow H_2 + H; \alpha = 4.6 \times 10^{-6} T_e^{-0.65}\ \mathrm{cm}^3\ \mathrm{s}^{-1}$$
$$H^+ + e^- \rightarrow H + h\nu; \alpha = 1.9 \times 10^{-10} T_e^{-0.7}\ \mathrm{cm}^3\ \mathrm{s}^{-1}$$

and at high pressures in these atmospheres, H atoms recombine quickly to recycle H_2, either directly,

$$H + H + M \rightarrow H_2 + M\ ;\ \mathrm{k} = 2.7 \times 10^{-31} T^{-0.6}\ \mathrm{cm}^6\ \mathrm{s}^{-1}$$

or catalytically through reactions involving hydrocarbons. Chapters I.2 and I.3 explore more fully the neutral and ion chemistry in the upper atmospheres of the giant planets.

6.2. Terrestrial CO_2 Atmospheres

The inner, terrestrial planets got a late start in formation because most hydrogen-bearing ices never condensed to solids in the hot, inner regions of the solar nebula. Consequently the terrestrial planets did not have as large a reservoir of solid material and could not grow as large as the giant outer planets and accrete gas and dust. Powerful solar winds after the formation of the protosun may have swept the inner solar system clean of gas and dust, leaving the late starting terrestrial planets with far less raw material for formation. Given the absence of substantial amounts of hydrogen, the terrestrial atmospheres emerged as strongly oxidizing in contrast to the strongly reducing atmospheres of the giant planets. On Venus the high surface pressure and temperature establish a chemical region in the lowest 10 km, where thermochemical processes predominate over photochemistry and carbonate rock can liberate CO_2. The inventory ratio of atmospheric N_2/CO_2 is comparable on the twin sister planets Venus and Earth. With the inclusion of CO_2 in Earth limestones, their absolute CO_2 abundances are also comparable. Although the present Earth does not have a CO_2 atmosphere, it would have one if either life never existed and/or its surface temperature were elevated to surface conditions comparable to Venus through the liberation of CO_2 from carbonate rock and evaporation of the oceans. On Mars the permanent CO_2 southern polar cap buffers its CO_2 atmosphere. The northern polar cap is mostly water ice. Venus is almost devoid of water, whereas Earth and Mars have large and moderate surface reservoirs, respectively.

Solar photolysis generates fast destruction rates of these CO_2 atmospheres:

$$CO_2 + h\nu(\lambda < 2000\text{Å}) \rightarrow CO + O;$$
$$\mathrm{J} = 1.2 \times 10^{-6}\ \mathrm{s}^{-1} \text{ at 1 AU}$$

which if followed only by

$$CO + O + M \rightarrow CO_2 + M;$$
$$\mathrm{k} = 6 \times 10^{-36}\ \mathrm{cm}^6\ \mathrm{s}^{-1}$$

and $O + O + M \rightarrow O_2 + M$;
$\mathrm{k} = 5 \times 10^{-35} \exp(900/\mathrm{T})\ \mathrm{cm}^6\ \mathrm{s}^{-1}$,

where the former reaction is spin-forbidden and slow, and the latter is fast, the result would be an irreversible conversion of CO_2 into CO and O_2 in only 4 million years in the massive Venusian atmosphere and only 4000 years in the Martian atmosphere. The stability of these atmospheres has been hypothesized, but not conclusively demonstrated, to be due to fast catalytic cycles involving the odd hydrogen compounds (H, OH, HO_2, HO_x) as discussed in Chapters I.2 and I.3. On Venus the HO_x is derived from H_2, which in turn is dissociated catalytically by Cl atoms liberated in HCl photolysis, whereas on Mars either photolysis of H_2O (wet phase) or H_2 oxidation by $O(^1D)$ from O_3 photolysis (dry phase) supplies HO_x.

The other topic of considerable interest on the terrestrial planets is the inventory, evolution, and escape of water and its photolysis products. The Earth, of course, has a liquid water ocean of approximate depth $\sim$ 3 km. Mars has a permanent northern, mostly water ice, cap and perhaps as much as a few hundreds of meters of water buried beneath the surface. In contrast Venus is essentially bone dry with only about 0.01 bar in its atmosphere and with a surface temperature of 730 K incapable of storing water in liquid or solid phase. Venus, the Earth's twin planet, is widely regarded to have undergone a runaway greenhouse based on the large enhancement ($\sim$ 100) of the D/H ratio derived from measurements of the [HDO]/[H_2O] ratio. Evaporation of a water ocean of depth comparable to our own ocean due to a runaway greenhouse coupled with water vapor photolysis and mass dependent escape rates of H and D could in principle account for the isotopic enhancement of deuterium as discussed in Chapters I.2 and III.2. The O atoms generated from photolysis subsequently oxidized surface rocks. Alternatively, the observed water vapor abundance is maintained in steady-state balance by cometary infall and photolysis of H_2O followed by nonthermal escape of hydrogen. Over the age of solar system there is no requirement of excess primordial water to explain the observed [HDO]/[H_2O] ratio[*Grinspoon and Lewis*, 1988].

In the CO_2 atmospheres of Venus and Mars, photoionization of CO_2 is the dominant source of ions

$$CO_2 + h\nu \rightarrow CO_2^+ + e\ ;\ \mathrm{I} = 6.6 \times 10^{-7}\ \mathrm{s}^{-1} \text{ at 1 AU}$$

The CO_2^+ reacts rapidly with atomic oxygen, which is abundant in the upper atmosphere, to form oxygen ions

$$CO_2^+ + O \rightarrow O^+ + CO_2\ ;\ \mathrm{k} = 1.6 \times 10^{-10}\ \mathrm{cm}^3\ \mathrm{s}^{-1}$$
$$CO_2^+ + O \rightarrow O_2{}^+ + CO\ ;\ \mathrm{k} = 9.6 \times 10^{-11}\ \mathrm{cm}^3\ \mathrm{s}^{-1}$$

with O^+ converted rapidly to O_2^+ by

$$O^+ + CO_2 \rightarrow O_2^+ + CO\ ;\ \mathrm{k} = 1.1 \times 10^{-9}\ \mathrm{cm}^3\ \mathrm{s}^{-1}$$

and ensuring that O_2^+ is the dominant, terminal ion in the ionospheres of Mars and Venus, as discussed in Chapter I.3.

6.3. N_2 Atmospheres

The last broad category is N_2 atmospheres. The emergence of life on the Earth led to the removal of CO_2 as the dominant gas and the ascent of N_2 as its prime atmospheric constituent with living organisms controlling the 21% O_2 content far from thermodynamic equilib-

rium by the processes of photosynthesis and respiration. The ocean supplies the dominant greenhouse gas, H_2O, and the most important oxidizing agent in atmospheric chemistry, the OH radical. Photochemistry of O_2 generates O_3, which sustains life by filtering out harmful solar UV before its reaches the surface. The cycle of O_3 absorbing solar radiation, dissociating to form O atoms, and the regeneration of O_3 by the reaction of O + O_2 with liberation of heat creates the thermal inversion region known as the stratosphere. In the thermosphere atomic oxygen emerges as the dominant constituent because, while photolytic destruction of O_2 is fast, no fast bimolecular reactions exist in the thermosphere to recycle O_2. Atomic oxygen recombination occurs only by downward diffusion to the mesopause region where catalytic reactions involving odd hydrogen supplemented by direct recombination O + O + M → O_2 + M lead to reformation of O_2. In contrast, molecular nitrogen is difficult to dissociate directly. Due to the absence of allowed transitions from its ground term into dissociating upper electronic terms, dissociation proceeds primarily by ionization first and then subsequent ion molecule reactions that break the N_2 bond. Atomic nitrogen does not emerge as an abundant component of the thermosphere, principally because N_2 is efficiently regenerated locally by the fast bimolecular reaction N + NO → N_2 + O, k = 3.1 x 10^{-11} cm^3 s^{-1}.

The earliest atmosphere on the Earth is speculated to have been mildly reducing with a composition similar to the present day atmosphere on Titan, the largest satellite of Saturn. Titan has the most massive N_2 atmosphere in the solar system at 1.4 bar and a surface temperature of 94 K. The next most abundant constituent is CH_4 with a volume mixing ratio of a few percent in the troposphere and ~ 2% above the tropopause. The combined photochemistry of N_2 and CH_4 leads to the formation of a large suite of hydrocarbons, organic molecules, and nitriles that condense to yield an optically thick haze that envelopes Titan and elevates its optical limb about 250 km above the surface. This photochemical smog is Titan's analog to the Earth's ozone, in that it absorbs solar radiation and heats Titan's stratosphere approximately 100 K above the tropopause temperature. The H and H_2 produced in CH_4 photolysis rapidly escape Titan's extended atmosphere and weak gravitational field, ensuring the irreversible destruction of CH_4 to heavier hydrocarbons and necessitating CH_4 resupply from the interior. In Titan's ionosphere the primary ions produced are N_2^+ and N^+, which react with CH_4 to initiate a chain of reactions that yield complex organic ions as the terminal ions in an atmosphere that contains a large assortment of organic molecules as discussed in Chapter I.3.

In the distant outer solar system, the planet Pluto and the largest Neptunian satellite Triton are widely regarded as the largest end-members of Kuiper-Belt objects that occupy the region from ~ 30 to 100s of AU, and serve as the source of short period comets. These "twin" objects have thin buffered N_2 atmospheres controlled by interactions with surface ice, primarily N_2 frost. Additional expected (CO) and detected (CH_4) atmospheric constituents are also controlled intimately by interaction with their surface frosts which may be well-mixed with the N_2 frost. Triton's surface pressure is ~ 14±1 μbar and surface temperature is ~ 38 K based on Voyager 2 data [*Yelle et al.*, 1995]. In the case of Pluto we know from the Infrared Space Observatory (ISO) that its surface is not isothermal [*Lellouch et al.*, 2000] and the surface pressure can be anywhere from at least ~ 3 μbar based on the *Elliot et al.* [1989] KAO stellar occultation data to possibly as large as 100 μbar if obscuring clouds and/or haze mask the surface location in the stellar occultation data. In fact our knowledge of Pluto's atmospheric composition is very limited with only a measurement of the CH_4 column density, ~ 3 x 10^{19} cm^{-2}, with large error bars from a near-IR solar reflection spectrum in the 1 μm region [*Young et al.*, 1997a]. Other species, in particular N_2 and CO, must be estimated from surface ice abundances and temperatures and the assumption of vapor pressure equilibrium. There are substantial differences in the atmospheres Pluto and Triton at the microbar level where stellar occultation measurements probe. Pluto's scale height and temperature are twice Triton's values [*Elliot et al.*, 2000].

The photochemistry of CH_4 in these atmospheres yields C_2H_4 and C_2H_2 which condense to form thin hazes, as observed by Voyager 2 on Triton, and eventually are deposited as frosts on the surface, but so far undetected on either object. Atomic and molecular hydrogen, products of methane photolysis, rapidly escape. The photochemistry of N_2 and CO lead to the formation of an ionosphere and nitriles and the production of C and N atoms, which can escape thermally. The dominant source of mass for Neptune's magnetosphere is escape of H, N, and H_2 from Triton and precipitation of energetic magnetospheric electrons may contribute two-thirds of the power input to Triton's upper atmosphere (cf. Table 1). Further discussion of these topics may be found in Chapters I.2, III.2, and IV.4.

6.4. *Volcanic Atmospheres*

The volcanic generated atmosphere of Io is in a class by itself. The innermost Galilean satellite is the site of the most active volcanism in the solar system. The volcanos are powered by tidal heating as a result of the Laplace resonance involving the orbital periods of Io, Europa, and Ganymede. The associated forces generate an eccentric motion for Io in the presence of Jupiter's enormous gravitational field with tidaling heating a natural consequence. The driving gases are SO_2, S_2, and maybe O_2 [*Zolotov and Fegley*, 1998]. SO_2, S_2, and SO are the principal components of its atmosphere [*Lellouch*, 1996; *Spencer et al.*, 2000]. SO_2 frosts are prevalent at mid and high latitudes and on the nightside where the surface temperature drops to ~ 95 K. At this temperature the vapor pressure of SO_2 is only 0.0004 nbar. A typical dayside surface pressure would be ~ 0.3 nbar. The fundamental question is whether the SO_2 atmosphere, which is preferentially confined to the equatorial regions, is a buffered atmosphere in equilibrium with a variable temperature surface frost or primarily an atmosphere formed by multiple volcanic plumes. Mass loss from Io's atmosphere by thermal escape, by heavy torus ion bombardment/sputtering of Io's atmosphere, exosphere, and surface [*McGrath and Johnson*, 1989] and by plasma pickup supplies copious amounts of oxygen, sodium, and sulfur to the Jupiter's inner magnetosphere. Also the torus plasma can be energized by charge exchange reactions involving neutrals in Io's atmosphere and exosphere. Torus electrons precipitate into the atmosphere and create a highly conducting ionosphere. Joule heating by Io's electrodynamic interaction with the Io torus plasma is the principal heating mechanism (cf. Table 1). Chapters II.1, II.2, and III.2 discusses these topics in much more detail.

6.5. *Sputter-Generated Atmospheres*

The next Galilean satellites Europa and Ganymede orbit also in the harsh environment of the inner Jovian magnetosphere. Their partial water ice surfaces are subjected to severe ion bombardment and ion induced ejection of substantial numbers of H_2O, H_2, and O_2 molecules off the surface (see Chapter III.3). Whereas H_2O sputtering rates are about 10 times the H_2 and O_2 rates, water is a condensible and hence has a large sticking coefficient, ~ 1. Neither H_2 nor O_2 are condensible and have much smaller surface sticking coefficients (~ 0.001). Thus H_2O emerges as a minor component of their atmospheres, in spite of its much larger sputtering rate which does not compensate for its unity sticking coefficient. The H_2 molecules escape readily from these satellites leaving behind the much heavier O_2 as the dominant atmospheric species. In the case of Europa there is an adequate first order description of the mass balance of the O_2 atmosphere [*Saur et al.*, 1998]. Europa's suprathermal torus ions, with a contribution from thermal ions, sputter O_2 from the water ice surface and thermal torus ions remove the O_2 atmosphere by sputtering with a net molecular flux of ~ 10^{27} O_2 s^{-1}. The resulting surface and column density just barely qualifies the gravitationally bound O_2 as an atmosphere with surface pressure of ~ 0.0007 nbar. Joule heating associated with ~ 1 x 10^6 Amps of ionospheric current is the dominant source of atmospheric heating (cf. Table 1). For Ganymede with its own internal magnetic field the inference of the O_2 column density and surface pressure is more complicated, but best estimates suggest comparable values to those appropriate for Europa [*Hall et al.*, 1998].

While Mercury and the Moon do not possess a conventional atmosphere, they do have tenuous alkali metal exospheres, principally Na, K, and Ca. These atoms execute ballistic orbits above the surface. These exospheres are discussed in depth in Chapter III.3.

6.6. *Comas*

In the vicinity of 1 AU, comas are predominantly water vapor. The photodissociation of H_2O is of fundamental importance.

$$H_2O + h\nu \rightarrow OH + H \ ; \ J = 1 \times 10^{-5} \ s^{-1} \text{ at 1 AU}$$
$$H_2O + h\nu \rightarrow H_2 + O(^1D) \ ; \ J = 1.4 \times 10^{-6} \ s^{-1} \text{ at 1 AU}$$

where in the first channel the H atom acquires the bulk of the excess energy and is ejected with a velocity of ~ 25 km s^{-1} in comparison to the OH speed ~ 1.5 km s^{-1} and the radial H_2O bulk speed of ~ 1 km s^{-1}. The fast moving H atoms lead to the generation of a large Lyman α halo by resonance scattering of solar Lyman α radiation with characteristic dimension ~ 10^7 km. Channel 2 proceeds at ~ 15% of the rate of channel 1 and produces an electronically excited, highly reactive O atom. Ionization of H_2O is the predominant source of ions

$$H_2O + h\nu \rightarrow H_2O^+ + e \ ; \ I = 3.3 \times 10^{-7} \ s^{-1} \text{ at 1 AU}$$
$$H_2O^+ + H_2O \rightarrow H_3O^+ + OH \ ; \ k = 2 \times 10^{-9} \ cm^3 \ s^{-1}$$

with conversion by the second reaction to H_3O^+ in the inner coma. Given the large suite of volatile minor constituents in the nucleus, the photochemistry of comas

involves an exceedingly large number of reaction paths and species as discussed in Chapter II.4.

7. THE THERMAL STRUCTURE OF THERMOSPHERES: THE ROLE OF MOLECULAR HEAT CONDUCTION

A survey of the atmospheres in our solar system, where we have some idea of their vertical temperature profiles, indicates upper atmospheres invariably have thermospheres with the fundamental properties of isothermal conditions near the exobase and a base region with steep temperature gradients. The latter implies substantial downward transport of heat by molecular conduction. The dominant molecules in most atmospheres are homonuclear (e. g. H_2, N_2, O_2) and thus have no permanent dipole moment and are infrared inactive with no rotational or vibrational absorptions/emissions. The terrestrial atmospheres of Venus and Mars do have the infrared active molecule CO_2 as their dominant constituent, yet still have thermospheres. (Venus has a dayside thermosphere, but not on the nightside, where the temperature decreases with increasing height, due to its slow rotation rate and long duration of a solar day - time between sunrises $\sim$ 117 Earth days.) In the presence of intense solar UV radiation CO_2 molecules are subjected to large photolysis rates and conversion to O and CO at high altitudes, with CO less susceptible to dissociation due to it large dissociation energy.

The exobase is located at column density depth, $1/\sigma \sim 3 \times 10^{14}$ cm^{-2}, whereas a typical atomic or molecular cross section for absorption of solar UV radiation is $\sim 10^{-17}$ cm^2 and hence typical penetration depth $\sim 10^{17}$ cm^{-2}, approximately 6 scale heights below the exobase. With no appreciable local radiative energy loss at the heights of maximum solar UV radiation deposition, the atmospheres must thermally conduct heat downward to the mesopause region where significant abundances of infrared active molecules are available and capable of radiating away the solar UV power deposited in the thermosphere.

The heat equation for low Mach number conditions, which ensures that c_p is the appropriate specific heat, is

$$\rho c_p \frac{\partial T}{\partial t} = -\frac{\partial}{\partial z}\left(-\kappa \frac{\partial T}{\partial z}\right) + Q_{UV} - C_{IR} \qquad (22)$$

where Q_{UV} = absorbed solar energy that is converted locally to heat, C_{IR} = infrared radiative cooling, and t = time. Now $\kappa = f \mu c_v$ from the kinetic theory of gases, where μ = coefficient of viscosity, c_v = specific heat at constant pressure, and f = Eucken's number = 2.5 for monotonic gases and ≤ 2 for diatomic gases.

In steady state $\partial T/\partial t = 0$, which also holds when Eq. (22) is averaged over a day. In averaging over a day, the flux must be reduced by 1/2 and the solar zenith angle set to $\bar{\mu}_0 = 1/2$. The global average is thus 1/4, as expected from intercepted solar flux of πr^2 and radiative cooling over $4\pi r^2$ area. Integrating (22) over time and altitude

$$\kappa \frac{\partial T}{\partial z} = \frac{1}{4}\int_z^\infty Q_{UV} dz - \int_z^\infty C_{IR} dz \qquad (23)$$

where the upper boundary condition is no net heat conducted into or out of the atmosphere $\frac{\partial T}{\partial z}|_\infty = 0$. Now $\kappa \partial T/\partial z$ is the downward heat conduction flux which is equal to the integrated heating rate above level z minus the integrated cooling rate. At high altitudes the UV optical depth is negligibly small and the atmospheric heating rate is proportional to the number density and thus decreases exponentially with increasing height. Likewise, C_{IR} is proportional to the number density of IR active molecules which are also exponentially decreasing with altitude. Equation (23) indicates $\kappa(\partial T/\partial z) \rightarrow 0$ and thus $T \rightarrow T_\infty$, the thermospheric temperature, which must be a constant temperature in the absence of additional heat sources or sinks. At lower heights, z, the temperature gradient must be sufficiently large to sustain a downward heat flow equivalent to the total UV energy absorbed above z less the IR radiative loss.

At the mesopause, $\partial T/\partial z = 0$ by definition and from (23), then

$$\frac{1}{4}\int_z^\infty Q_{UV} dz = \int_z^\infty C_{IR} dz \qquad (24)$$

i.e., the integrated UV heating above the mesopause is precisely balanced by the IR cooling. The location of the mesopause occurs at an altitude where the entire downward heat conduction flux is radiated away in the IR.

A simple illustrative model can be constructed, if all the thermospheric heating occurs at a single height, z_q, or pressure level, p_q, with a delta function source $Q_0\delta(p - p_q)$ in pressure coordinates. Similarly, assume all the IR cooling occurs at single height/pressure z_c, p_c, with delta function sink $C_0\delta(p - p_c)$. By definition of the mesopause, Eq. (24) is satisfied when the lower limit of integration is slightly below the height, z_c, where $p = p_c$, i. e., to z_c^-. Substitution of these approximations into Eq. (22) for steady state conditions and integration over the following regions give

$$\begin{aligned} &\text{if } 0 < p < p_q \quad T = T_\infty = T(p_q) \\ &\text{if } p_q < p < p_c \quad T(p)^{s+1} = T_c^{s+1}(p_c) \\ &\qquad - \frac{(s+1)F_{HC}H}{A} ln\left(\frac{p}{p_c}\right) \end{aligned} \qquad (25)$$

where T_∞ is the isothermal temperature in the upper thermosphere, T_c is the "cooling" temperature at the mesopause, the thermal conductivity κ is accurately approximated by AT^s, F_{HC} is the downward heat conduction flux $|-AT^s dT/dz|$ and equal to Q_0, H is the pressure scale height which is assumed constant for integration purposes. One can rewrite (25) in height coordinates by noting that -H $ln(p/p_c)$ is just $z - z_c$. The quantities F_{HC} and Q_0 are equal to the integrated thermospheric absorption rate of solar UV and EUV radiation times the efficiency factor for conversion into heat. CO_2 absorbs solar UV radiation out to 2000 Å, whereas O_2, N_2, O, and H_2 absorb below 1750, 1000, 911, and 1100 Å, respectively. Although there are some planetary variations in fractions of the solar UV spectrum absorbed and heating efficiencies, the largest variation is the solar flux decrease with inverse distance squared. Whereas the integrated globally average heating rate in the Earth's thermosphere is a few erg cm^{-2} s^{-1}, it is only $\sim$ 0.01 erg cm^{-2} s^{-1} on Jupiter and a miniscule 0.0004 erg cm^{-2} s^{-1} at Neptune in their H_2 dominated atmospheres, as may be inferred from Table 1. Thus the thermal structure of the terrestrial planets can be understood in terms of solar UV heating, whereas in the giant planets' thermospheres it is a negligible heat source, as outlined below and treated in much greater depth in Chapters IV.1 and IV.2.

The depth of solar EUV and UV penetration for the purposes of heating calculations can be obtained by a suitable wavelength average of the absorption cross section weighted with photon energy, $< \sigma_\lambda >$. Its inverse is the penetration column density corresponding to pressure level $p_q = mg/ < \sigma_\lambda >$. For the H_2 dominated atmospheres of the giant planets, $< \sigma_\lambda > \sim 10^{-18}$ cm^2 and the mesopause is approximately at the 1 μbar level. With the integrated globally averaged heating rates given above, Eq. (25) yields for the temperature contrasts $[T(p_q) - T_c(p_c)] \sim$ 60, 30, 20, and 4 K for Jupiter, Saturn, Uranus, and Neptune, respectively. These temperature differences between the high altitude isothermal region and the mesopause region are substantially smaller than the values inferred from Voyager UV solar occultation measurements, rotational structure of H_3^+ near-IR emission, and in the case of Jupiter from Galileo probe deceleration data. Table 1 gives T_∞ for solar system objects and Fig. 1 conveys the approximate temperatures at their mesopauses.

Given the inadequacy of solar heating to account for thermal thermospheric structure on the giant planets, a number of suggestions have been made over the years with specific application to Jupiter: soft electron precipitation, energetic electrons, joule heating, gravity wave dissipation, and heavy ion precipitation (for references, see *Matcheva and Strobel*, 1999). Power input to thermospheres of the giant planets by particle precipitation and Joule heating can be substantial as indicated in Table 1. Most recently, the gravity wave heating suggestion has received the most attention, due in large part to the inference of large scale gravity waves in the Galileo probe deceleration data [*Young et al.*, 1997b; *Matcheva and Strobel*, 1999; and *Hickey et al.*, 2000]. The latter two papers concluded that gravity waves at the observed amplitudes in the probe data cannot account for Jupiter's thermospheric temperature profile.

8. WAVE HEATING: WHY DON'T ALL ATMOSPHERES HAVE CORONAS?

Wave heating of the solar corona has been a popular explanation for its very elevated temperatures ($> 10^6$ K), but has never gained universal acceptance. *Hines* [1965] was a strong advocate of gravity wave heating playing an essential role in the energetics of the Earth's upper atmosphere. But as discussed in Chapters I.2 and IV.1, solar EUV and UV heating plus approximately a 15% contribution from auroral power dissipation adequately accounts for the power input to the Earth's thermosphere. Wave and tidal coupling on Venus and Mars are discussed in Chapter III.1. Because gravity waves are ubiquitous in planetary atmospheres and can transport significant energy fluxes by vertical propagation from excitation sources in the lower atmosphere, why is it not inevitable that all planetary atmospheres have hot coronas?

Gravity waves have angular frequencies, $\omega = k_h c$, bounded on the low end by the coriolis frequency, $f = 2\Omega sin(\theta)$ and on the high frequency side by the buoyancy frequency [*Andrews et al.*, 1987; *Gill*, 1982]. Here Ω is the planet's rotation rate, k_h is the horizontal wave number, c is the horizontal wave phase speed, and θ is the latitude. For a dry atmosphere with low Mach number flow, the buoyancy frequency is $N = [(g/T)(dT/dz + g/c_p)]^{1/2}$. From observations in the Earth's atmosphere most of the gravity wave power re-

sides in hydrostatic gravity waves [*Fritts*, 1984] which obey the condition $(Hk_h^2(\bar{u}-c)^2/g \ll 1$ which is equivalent to $\omega^2 \ll N^2)$, where $\bar{u}$ is the mean zonal wind [*Andrews et al.*, 1987; *Gill*, 1982]. In addition, these hydrostatic gravity waves satisfy in many instances the further restriction in the dispersion relation known as the "Boussinesq" approximation $k_z^2 \gg 1/4H^2$ [*Andrews et al.*, 1987], where k_z is the vertical wave number. The physical meaning is the atmospheric density variation may be assumed approximately constant over one vertical wavelength, but not many scale heights. Radio and stellar occultation measurements of gravity wave spectra in other atmospheres confirm this conclusion.

The vertical transfer of energy and momentum by gravity waves requires that the ratio of group velocities $c_{gz}/c_{gh} \approx (\omega^2 - f^2)^{1/2}/N \approx k_h/k_z$ [e. g. *Andrews et al.*, 1987], should not be too small or otherwise most of the gravity wave excitation energy will be dispersed in the horizontal direction, h, rather than the vertical direction, z. This requires that $\omega^2 \gg f^2$, i. e., the wave period should not be too close to the inertial period.

Gravity wave amplitudes grow approximately exponentially with upward propagation because the Eliassen-Palm flux ($F = c_{gz}A$) is conserved in the absence of dissipation according to the generalized Eliassen-Palm theorem [*Andrews et al.*, 1987], where

$$c_{gz} = \frac{Nk_h}{k_z^2}, A = -k_h\left(\frac{E}{\hat{\omega}}\right); \quad (26)$$

$$E = \tfrac{1}{2}\rho_0\left[\overline{u'^2} + \overline{v'^2} + \overline{w'^2} + \frac{N^2\overline{w'^2}}{k_h^2(\bar{u}-c)^2}\right]$$

Here $\hat{\omega} = \omega - k_h\bar{u}$ is the intrinsic or Doppler-shifted frequency, A is wave action, E is the total wave energy (or energy density), and $E/\hat{\omega}$ is the wave action density [*Andrews et al.*, 1987]. Wave energy is only strictly conserved in the absence of dissipation when $\bar{u}$ is constant. For slowly varying $\bar{u}$ with height, the monochromatic gravity wave amplitude increases with height approximately as $(\rho_0)^{-0.5}$. There is a limit to this exponential growth known as gravity wave saturation and also referred to as wave breaking. Saturation occurs when the wave drives the local temperature lapse rate (i. e., the sum of the wave and mean state temperature lapse rates, denoted by prime and subscript zero, respectively) adiabatic [*Lindzen*, 1981]. When this criterion is met the local buoyancy frequency goes to zero and locally the wave can no longer propagate because the buoyancy restoring force vanishes. For monochromatic hydrostatic gravity waves there are two other equivalent definitions that yield the same maximum amplitude: 1) the wave becomes nonlinear in the reference frame moving with the fluid velocity $\bar{u}$, and 2) the rate of vertical parcel displacement equals the vertical group velocity [*Fritts*, 1984; *Leovy*, 1982]. Mathematically the wave saturation criteria are:

$$|\tfrac{dT_0}{dz}| + |\tfrac{dT'}{dz}|_{sat} \geq \tfrac{g}{c_p}, T'_{sat} = \tfrac{N^2T_0}{gk_z} \quad (27)$$

$$|u'|_{sat} \geq |\bar{u}-c|, |w'|_{sat} \geq c_{gz} = \tfrac{k_h|\bar{u}-c|}{k_z}$$

To obtain the largest gravity wave heating in the thermosphere, gravity waves need to propagate through the stratosphere and mesosphere without reaching saturation amplitudes. If a wave breaks it dissipates wave energy and deposits momentum in the saturation zones and does not carry energy and momentum to much higher altitudes. Forcing a gravity wave with too large an amplitude in the lower atmosphere is counterproductive in heating the thermosphere as the wave saturates and dissipates in the middle atmosphere. If the wave reaches the thermosphere and is still at sub-saturation amplitude, then molecular viscosity acts to dissipate the wave energy with the wave reaching a maximum amplitude at the level where wave dissipation cancels exponential $(\rho_0)^{-0.5}$ amplitude growth

$$k_{zi} \approx \frac{1}{2H}, \text{where } k_{zi} \approx k_{zr}\left(\tfrac{\omega_i}{\omega_r}\right) \approx \tfrac{\mu}{\rho_o}\omega k_z^3 \quad (28)$$

when the WKBJ approximation is valid [*Matcheva and Strobel*, 1999]. Here subscripts r, i denote real and imaginary parts. Now the dispersion relation for "Boussinesq" hydrostatic gravity waves is $\omega \approx NK_h/k_z$ and (28) yields the mass density of the atmosphere, ρ_q, where the gravity wave reaches peak amplitude

$$\rho_q \approx 2H\mu\frac{k_z^4}{Nk_h} \quad (29)$$

The vertical gravity wave energy flux, F_{Ez}, is

$$F_{Ez} = Ec_{gz} \approx \frac{1}{2}\rho_q\frac{g^2}{N^2}|\frac{\omega}{k_z}|\frac{\overline{T'^2}}{T_0^2} \quad (30)$$

and reaches its maximum value at the saturation amplitude

$$F_{Ez} \approx \tfrac{1}{2}\rho_q\tfrac{N^3k_h}{k_z^4} \approx \mu HN^2 \rightarrow \tfrac{\mu gR}{c_p}, \quad (31)$$

$$\text{if T = constant}$$

Note that these expressions depend only on the background properties of the atmosphere and not explicitly on any wave properties which are embedded in expression (29) for ρ_q. The wave amplitude squared grows as ρ_0^{-1} until the wave amplitude saturates or viscous dissipation retards further wave growth. The maximum gravity wave energy flux is proportional to the background atmospheric mass density and its value will decrease exponentially with height when the wave reaches saturation amplitude.

With appropriate values for the input parameters, μ, g, and c_p/R, the maximum gravity wave energy fluxes in isothermal thermospheric regions for the terrestrial planets Venus, Earth, and Mars are 0.02, 0.1, and 0.01, respectively; for the giant planets Jupiter, Saturn, Uranus, and Neptune 0.13, 0.04, 0.04, and 0.04, respectively, and 0.0004 for Pluto in units of erg cm^{-2} s^{-1}. For the terrestrial planets these values are small in comparison to solar EUV and UV heating rates, whereas for the giant planets these values exceed substantially the solar heating rates. From the Galileo probe data the inferred downward heat flux by thermal conduction was ~ 0.5 erg cm^{-2} s^{-1}, or four times the maximum heating rate.

Larger gravity wave energy fluxes are possible in the lower thermosphere where the temperature gradients are large and positive (and also if viscous dissipation is not severe at the wave's vertical wavenumber, k_z, as noted above). In Eq. (31), H is now the density scale height given by $H[1 + (H/T)(dT/dz)]^{-1}$. For Jupiter's lower thermosphere this increases the maximum gravity energy flux to ~ 0.2 erg cm^{-2} s^{-1}. But for gravity wave heating to contribute substantially to high thermospheric temperatures the maximum wave dissipation must occur high in the thermosphere where the transition from significant temperature gradient to isothermal conditions takes place. This is imperative in order to achieve a large separation between heat input and radiative cooling and maintain a considerable temperature gradient over an extended altitude range, as is evident from Eq. (25). To attain maximum energy dissipation at high altitudes, Eq. (29) demands large vertical wavelengths/very small vertical wavenumbers because $\rho_q \propto k_z^3$. Physically, waves with large vertical wavelengths suffer smaller dissipation per unit distance and hence propagate to higher altitudes. However the WKBJ approximation breaks down for these waves and is suggestive that wave reflection may be important as *Hickey et al.* [2000] discuss. In addition, gravity waves induce a downward eddy heat flux, $c_p\overline{w'T'}$, that has the net result of lowering the effective altitude of wave dissipation [*Matcheva and Strobel*, 1999].

Finally, one might think that multiple gravity waves could supply the required thermospheric heating. However, finite amplitude waves can destructively interfere with one another and cause a wave to saturate much lower in the atmosphere. In a region where one wave has large negative dT'/dz, the local static stability is reduced substantially and may cause another wave to saturate at a much smaller amplitude and lower in the atmosphere than would occur in the absence of other waves. Thus the above values should be considered upper limits to gravity wave heating with viable values being somewhat less in magnitude.

The other important class of vertically propagating internal waves are Rossby waves whose restoring force is the meridional variation of the coriolis force and whose dynamics are based on linearized equations for conservation of potential vorticity, q [*Andrews et al.*, 1987]. Generally the potential vorticity of the atmosphere is dominated by planetary vorticity (the coriolis parameter defined above), f, with a minor contribution from relative vorticity of the velocity field, $\nabla \times \vec{v}$. As Rossby waves propagate vertically they must extract potential vorticity from the mean flow, q_0, in order for their wave potential vorticity, q', to grow exponentially in amplitude as $\rho_0^{-1/2}$, in the absence of dissipation. As *Schoeberl and Lindzen* [1982] demonstrated, the wave potential vorticity cannot exceed the basic state potential vorticity, i. e., $q' < f$ and this restricts wave amplitudes to two orders of magnitude lower than estimated by $\rho_0^{-1/2}$ amplitude growth. Because Jupiter's f is only ~ 2.5 times the terrestrial value, it is improbable that Rossby waves can produce either a hot terrestrial or a hot Jovian corona.

Acknowledgments.
Table 1 and Figure 1 are based on Table 4.2 and Figure 4.4 from AN INTEGRATED STRATEGY FOR THE PLANETARY SCIENCES 1995-2010, National Academy Press, Washington, DC. In addition the author's discussion on Composition and Chemistry is based on his contribution on pp. 113-117 from this report and used with permission. Partial support by NASA Grant NAG-5-4168 is acknowledged.

REFERENCES

Andrews, D. G., J. R. Holton, and C. B. Leovy, Middle Atmosphere Dynamics, Academic Press, Orlando, Chapter 4, 1987.

Chamberlain, J. W. and D. M. Hunten, Theory of Planetary Atmospheres, Academic Press, Orlando, Chapter 2, 1987.

Chapman, S., The Thermosphere - The Earth's Outermost Atmosphere in Physics of the Upper Atmosphere, ed. J. A. Ratcliffe, Academic Press, New York, p. 4, 1960.

Colegrove, F. D., F. S. Johnson, and W. B. Hanson, Atmospheric Composition in the lower thermosphere, *J. Geophys. Res.*, *71*, 2227-2236, 1966.

Delsemme, A. H. and D. C. Miller, Physico-chemical phenomena in comets, III. The continuum of Comet Burnham., *Planet Space Sci.*, *19*, 1229-1258, 1971.

Elliot, J. L., E. W. Dunham, A. S. Bosh, M. Slivan, L. A. Young, L. H. Wasserman, and R. L. Millis, Pluto's atmosphere, *Icarus*, *77*, 148-170, 1989.

Elliot, J. L., D. F. Strobel, X. Zhu, J. A. Stansberry, L. H. Wasserman, and O. G. Franz, The Thermal Structure of Triton's Middle Atmosphere, *Icarus*, *143*, 425-428, 2000.

Fritts, D. C., Gravity wave saturation in the middle atmosphere: A review of theory and observations, *Rev. Geophys. Space Phys.*, *22*, 275-308, 1984.

Gill, A. E., Atmosphere-Ocean Dynamics, Academic Press, New York, Sec. 8.4, 1982.

Grinspoon, D. H., and J. S. Lewis, Cometary water on Venus: implicatons of stochastic impacts, *Icarus*, *74*, 21-35, 1988.

Hall, D. T., P. D. Feldman, M. A. McGrath, and D. F. Strobel, The far-ultraviolet oxygen airglow of Europa and Ganymede, *Astrophys. J.*, *499*, 475, 1998.

Hickey, M. P., R. L. Walterscheid, and G. Schubert, Gravity wave heating and cooling in Jupiter's thermosphere, *Icarus*, *148*, 266-281, 2000.

Hines, C. O., Dynamical heating in the upper atmosphere, *J. Geophys. Res.*, *70*, 177, 1965.

Landau, L. D., and E. M. Lifshitz, Fluid Mechanics, Pergamon Press, New York, 1959.

Lellouch, E., Io's atmosphere: Not yet understood, *Icarus*, *124*, 1-21, 1996.

Lellouch, E., R. Laureijs, B. Schmitt, E. Quirico, C. de Bergh, J. Crovisier, and A. Coustenis, Pluto's Non- Isothermal Surface, *Icarus*, *147*, 220-250, 2000.

Leovy, C. B., Control of the homopause, *Icarus*, *50*, 311-321, 1982.

Lindzen, R. S., Turbulence and stress owing to gravity wave and tidal breakdown, *J. Geophys. Res.*, *86*, 9707-9714, 1981.

Matcheva, K. I., and D. F. Strobel, Heating of Jupiter's thermosphere by dissipation of gravity waves due to molecular viscosity and heat conduction, *Icarus*, *140*, 328-340, 1999.

McGrath, M. A., and R. E. Johnson, Magnetospheric plasma sputtering of Io's atmosphere, *Icarus*, *69*, 519-531, 1989.

Saur, J., D. F. Strobel, and F. M. Neubauer, Interaction of the Jovian Magnetosphere with Europa: Constraints on the Neutral Atmosphere, *J. Geophys. Res.*, *103*, 19,947-19,962, 1998.

Schoeberl, M. R., and R. S. Lindzen, A note on the limits of Rossby wave amplitudes, *J. Atmos. Sci.*, *39*, 1171-1174, 1982.

Spencer, J. R, K. L. Jessup, M. A. McGrath, G. E. Ballester, and R. V. Yelle, Discovery of Gaseous S2 in Io's Pele Plume, *Science*, *288*, 1208-1210, 2000.

Strobel, D. F. and B. C. Wolven, The Atmosphere of Io: Abundances and Sources of Sulfur Dioxide and Atomic Hydrogen, *Astrophys. Space Sci.*, *277*, 271-287, 2001.

Summers, M. E., D. F. Strobel, Y. L. Yung, J. T. Trauger, and F. Mills, The Structure of Io's Atomic Corona and Implications for Atmospheric Escape, *Astrophys. J.*, *343*, 468-480, 1989.

Yelle, R. V., J. I. Lunine, J. B. Pollack, and R. H. Brown, Lower Atmospheric Structure and Surface-Atmosphere Interaction on Triton, in Neptune and Triton, ed. D. P. Cruikshank, University of Arizona Press, Tucson, pp. 1031-1106, 1995.

Young, L. A., J. L. Elliot, A. Tokunaga, C. de Bergh, and T. Owen, Detection of Gaseous Methane on Pluto, *Icarus*, *127*, 258, 1997a.

Young, L. A., R. V. Yelle, R. E. Young, A. Seiff, and D. B. Kirk, Gravity waves in Jupiter's thermosphere, *Science*, *276*, 108-111, 1997b.

Zolotov, M. Y., and B. Fegley, Jr., Volcanic production of sulfur monoxide (SO) on Io, *Icarus*, *132*, 431-434, 1998.

D. Strobel, Departments of Earth and Planetary Sciences and Physics and Astronomy, The Johns Hopkins University, Baltimore, MD 21218-2687. (email: strobel@jhu.edu)